

PRODUCTION OF SECONDARY BEAMS AT THE CERN PROTON SYNCHROTRON

H. FISCHER and W. RICHTER
CERN, Geneva, Switzerland
(Presented by W. Richter)

I. INTRODUCTION

The following general characteristics of the CERN proton synchrotron have determined the production of secondary beams. About 2×10^{11} protons are accelerated to energies up to 28 Gev per cycle; the beam diameter, at the end of acceleration, is about 8 mm. The beam can be moved radially within a range of 70 mm and the reproducibility of its radial position, from cycle to cycle, is of the order of 0.2 mm.

For bubble-chamber experiments, secondary beams of 1 ms or less are produced either by flipping a target rapidly into the beam or kicking the latter onto a target, with partial or full consumption of the primary beam.

For counter experiments, on the other hand, long bursts of 100 ms and more are produced by spiralling the debunched beam against the target. During the last year, the proton beam was successfully kept circulating at full energy during a so-called "flat top" of the magnetic field. To assure a well-defined and reproducible magnetic field during the flat top, a "mean-speed regulation" of the magnets' power-supply generator had to be developed. The mean speed is held constant within ± 0.01 percent and the proton energy is then reproducible within ± 0.1 percent. Secondary beams with an intensity nearly constant for ≤ 500 ms can be obtained and at the same time the influence of the CPS magnet's stray field on the secondary beams is stabilized.

A universal target with two independent flip targets was developed, and it can be fitted into any of the 100 pump manifolds around the machine (Fig. 1).

II. SHORT BURST PRODUCTION

Three methods are used to produce bursts of 1 ms and less.

(a) The beam is kicked onto a thick target by excitation of free betatron oscillations. This method, using an 80-gauss deflection field of high frequency ("radio-frequency knock out")¹, gives full beam consumption within 100 to 300 μ s.

(b) A thin target finger (Figs. 1 and 2) cuts through the beam at a speed of about 30 mm/ms. This method gives 1- to 35-percent beam consumption within 300 to 800 μ s and leaves the remaining part of the beam for a long burst later in the cycle.

(c) The beam is rapidly brought onto a thick target by use of the beam jump, which is caused by the energy loss during the traversal of a fast target finger (Fig. 2) somewhere else in the machine and simultaneous beam-steering with radio frequency. This method is especially used for the production of 1-ms bursts from a point-source target where the actual target should not be moved.

III. LONG BURST PRODUCTION

A. Improvement of the Magnet Field Stability (mean-speed regulation)

Because no flat-top operation was provided originally, the top value of the magnetic field, and therefore also the proton energy, could drift by as much as ± 2 percent. To reduce this drift considerably, it was found that the mean speed of the magnets' power-supply generator must be kept constant to better than ± 0.1 percent. This is because the time of switching off the static converters at the end of

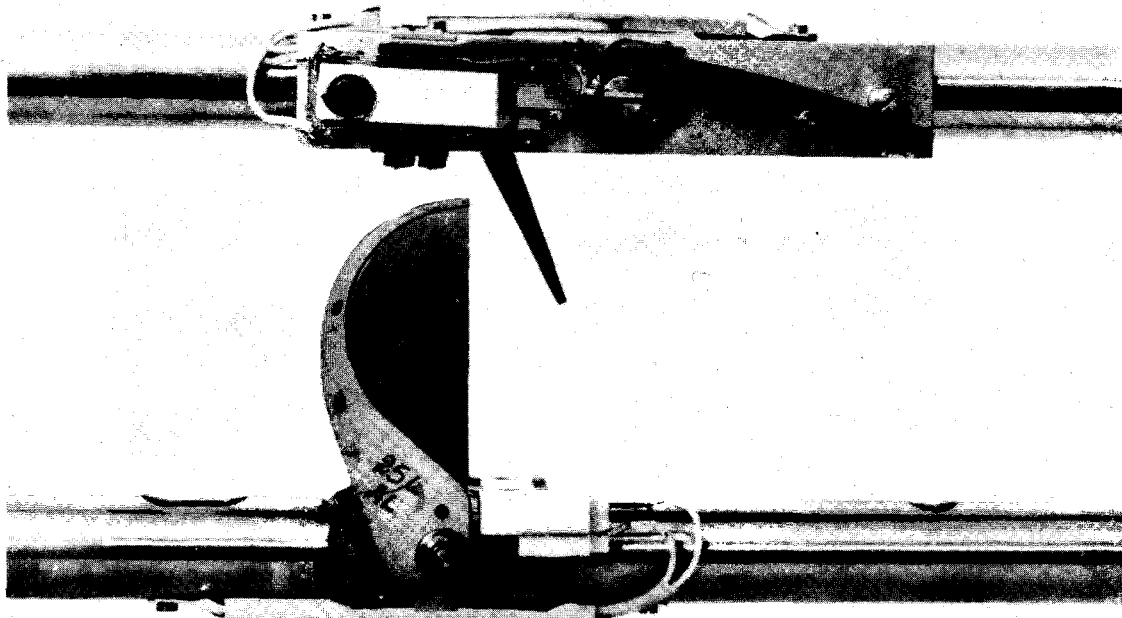
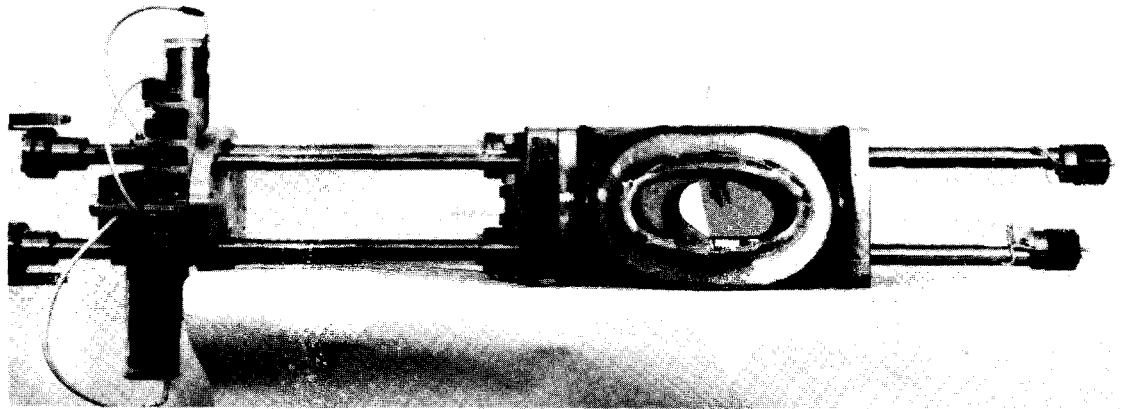


Fig. 1 Target unit. *Above*: targets mounted in pump manifold. Target heads are seen through the clearance of the vacuum chamber; pulling magnets are on the right, motor-drive for change of radial position on the left. *Below*: the actual targets enlarged. Long-burst foil target is on the bottom rod; short-burst fast target on the top rod.

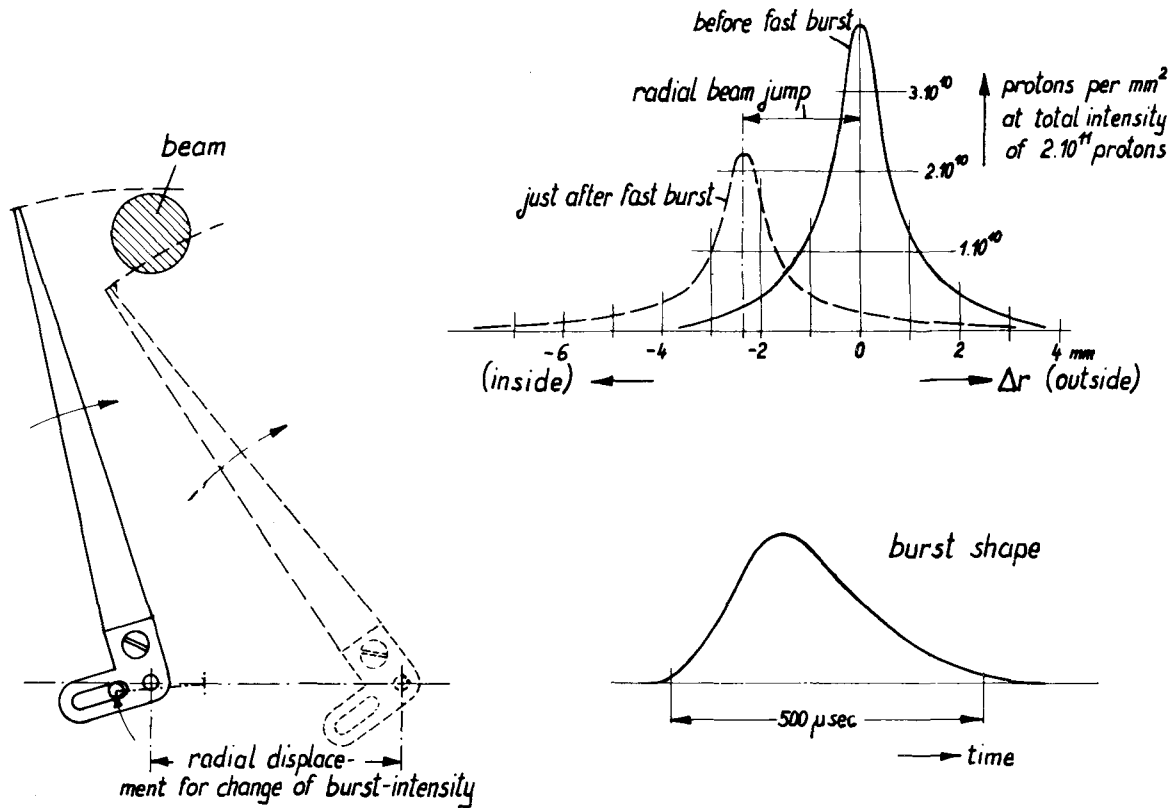


Fig. 2 Short-burst target.

the field rise is related to the phase of the generator voltage (i.e., the mean speed), whereas the magnet voltage had already a reproducibility better than ± 0.1 percent. Instantaneous values of this speed vary, periodically, by as much as ± 3 percent during one machine cycle.

The mean speed ω (averaged over one machine cycle) depends on the energy balance during this time and its relation to the energy E stored in the flywheel

$$\frac{\Delta\omega}{\omega} = \frac{\Delta E}{2E}$$

where ΔE is the difference between the energy E_M fed into the flywheel system during one machine cycle and the energy dissipation in the whole magnet's power-supply system during this time. In order to calculate the mean-speed error $\Delta\omega$, the variations of these energies have to be estimated. Considering that only short-term variations will limit the precision of the

regulation, the following quantities can be estimated:

(a) The motor input power which is kept constant by means of a power regulation using cascaded machines²; with normal variations in the mains' voltage, the error is kept below 0.1 percent corresponding to $\leq 10^4$ joule.

(b) The most important energy dissipation occurs in the magnet coils (Fig. 3). With the formulas given in the Appendix and with the specified jitter of the magnet voltage of ± 0.1 percent, the energy variation is 3×10^4 joule.

(c) The variation in energy dissipation in the static converters, in the machines and transformers, as well as in the bearings and ventilators, is negligibly small if constant mean speed is assumed.

With the sum of the energy variations ΔE , mentioned above, and the energy stored in the flywheel of $E = 1.5 \times 10^8$ joule, the estimated mean-speed variation should be

$$\Delta\omega/\omega = \Delta E/2E = \pm 1.3 \times 10^{-4}.$$

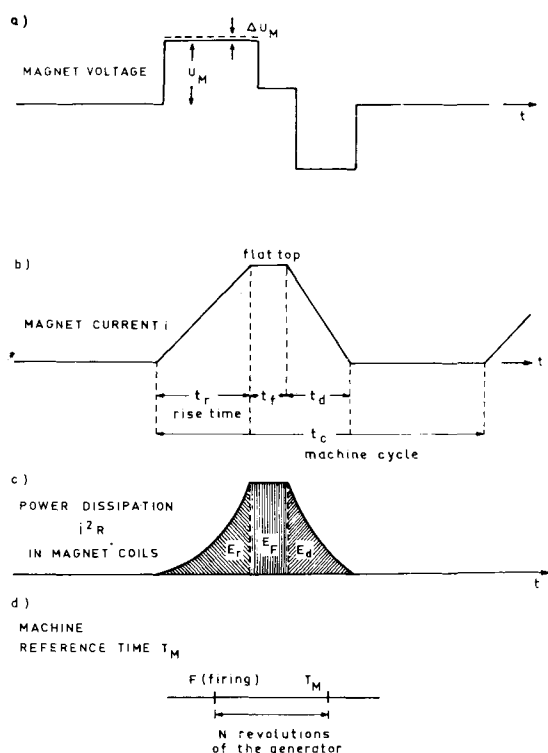


Fig. 3 Machine cycle of CPS; repetition rate, once every 3 seconds for 24 Gev top energy.

To reach the required measuring accuracy of 10^{-5} , the mean-speed regulation has been divided into a rough regulation which corrects time errors $\geq \pm 5$ ms, and a fine regulation which corrects errors of $< \pm 5$ ms and which is switched off when the error exceeds this value (Fig. 4). As the measuring time is about 1 second, 5 ms correspond to 0.5 percent.

Both regulators produce voltages proportional to the error and proportional to the time integral of this error, the sum of which represents the reference voltage for the power regulation with cascaded machines. This means the input power of the motor is regulated in order to keep the mean speed constant (Fig. 5).

B. Long-Burst Targeting

Three standard target types are now in general use:

(a) foil targets of Be or Al with normal thickness of 50μ ;

(b) vertical wire targets of Al with 0.5 mm by 0.5 mm cross section;

(c) point-source targets of about 3 mm diameter made of Be or Al wire pointing in the direction of the secondary beam.

The last type is required for secondary beams with separators needing a very small source.

All of these long-burst targets are flipped into a position close to the outer radius of the beam just at the beginning of the flat top. At the same time, the beam is debunched by stopping acceleration. The field over the flat top is made to decrease slightly so that the beam spirals on to the target. The burst length can be adjusted by altering the rate of this decrease. The mean-speed regulation has now improved the target operation considerably:

(a) The particle energy is reproducible from pulse to pulse within ± 0.1 percent;

(b) the influence of the CPS magnetic stray field on the secondary beams is kept within ± 0.1 percent;

(c) the rate of field decrease during the flat top is stable to ± 10 gauss/sec;

(d) the intensity of secondary particles during the burst can be maintained almost constant even with a flat-top slope of only 35 gauss in 200 ms.

For the time being, there is still a modulation on all the burst shapes, due to the 600-cycle magnet-current ripple. However, this will be suppressed by using a filter during the flat top.

In order to compare different target heads (e. g., different materials or different shapes), a six-head target has been developed (Fig. 6). With this mechanism, the heads can be interchanged between machine cycles according to a preselected sequence. This is done by a small motor via a special gear. The beam hits all the targets at the same azimuthal and radial position.

Furthermore, foil targets have been used which have a total weight (including frame) of 1 g and cover almost the complete vacuum-chamber cross section. The time for moving such a target through the beam is small compared with the total burst time. A $5\text{-}\mu$ aluminum foil has given a burst length of 200 ms which corresponds to 10^5 traversals or a total path through material of 500 mm. This value is about twice the nuclear mean-free-path

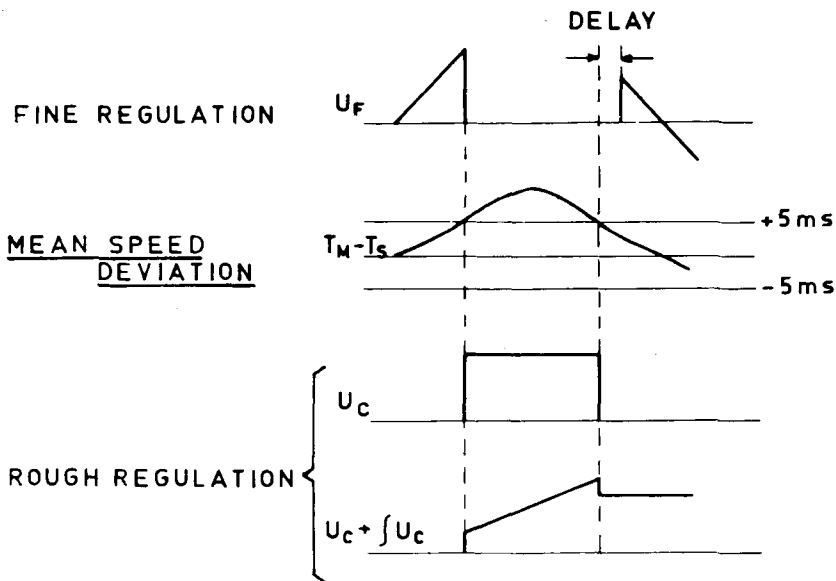
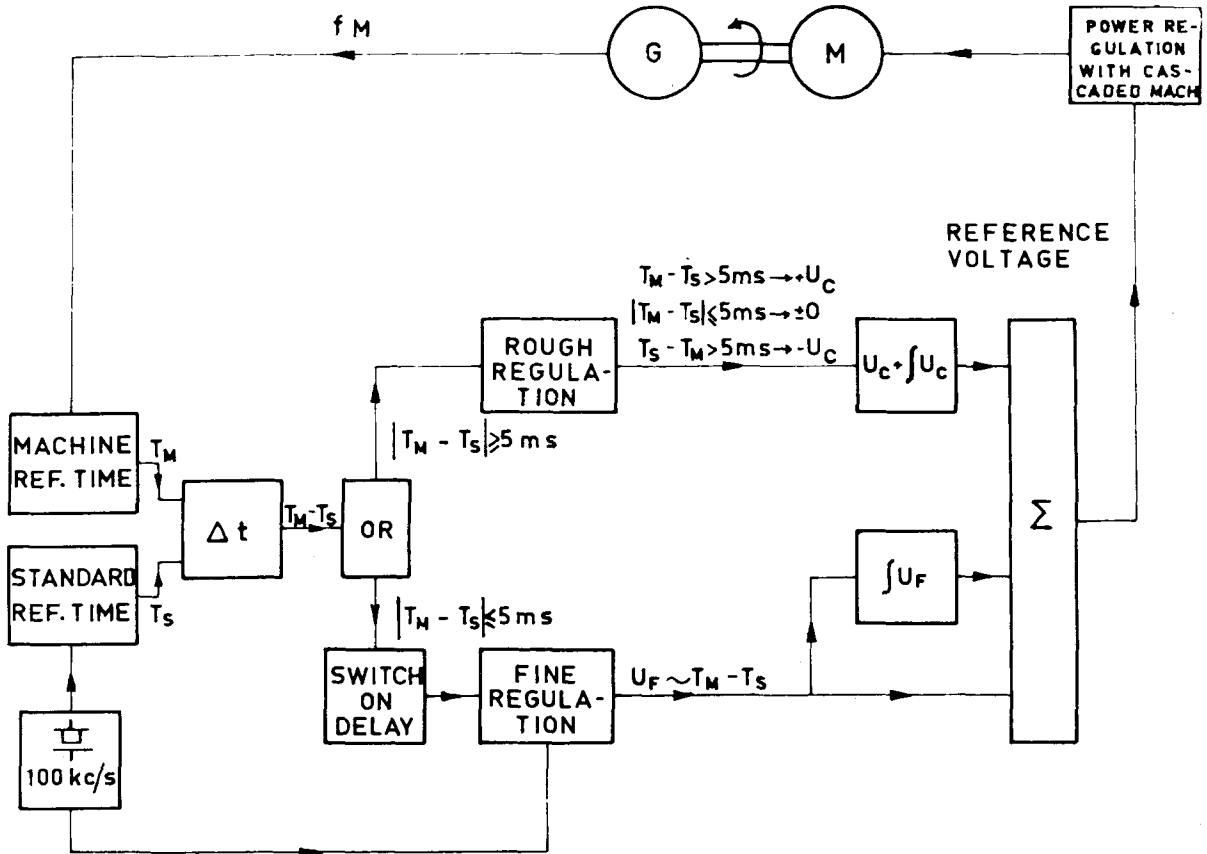


Fig. 4 Mean speed regulation; block diagram.

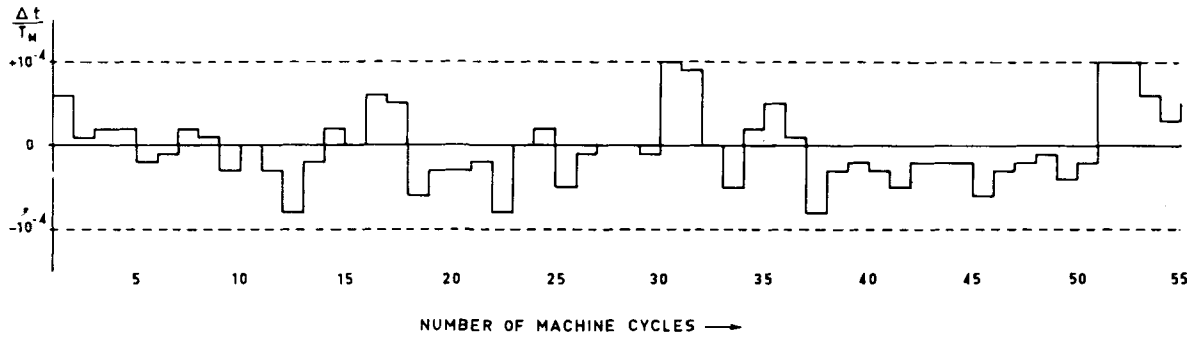


Fig. 5 Mean-speed regulation stability of machine; reference time T_M .

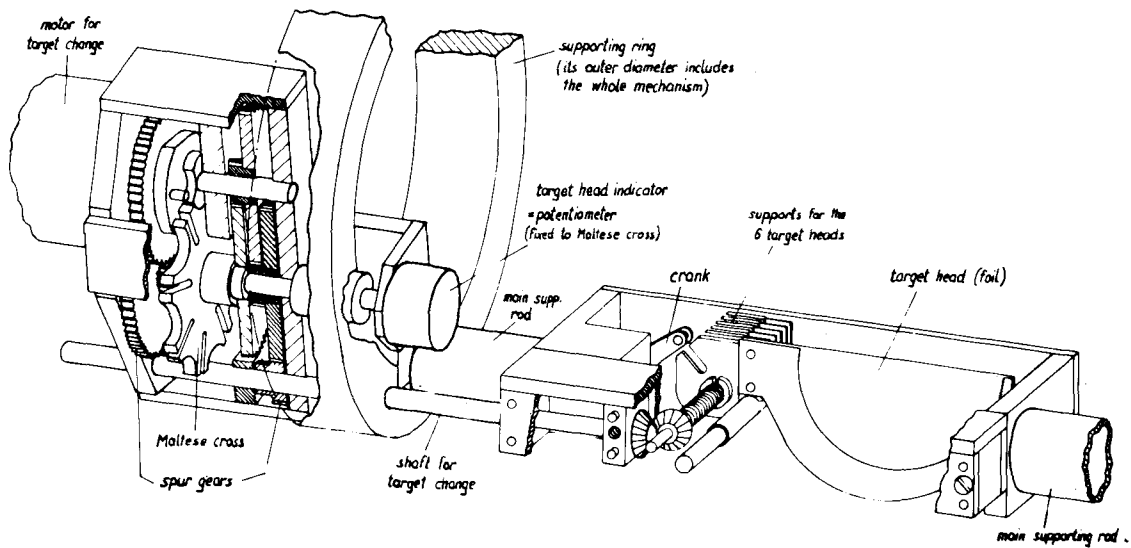


Fig. 6 Mechanism of six-head target. The magnet, which pulls the target by turning the crank, is not shown. All electrical connections and contacts (security devices) are ignored.

length, which is known to be 270 mm for this material. First results of efficiency for the large foil targets, which should be the most efficient ones, have been about 60 percent³.

IV. BEAM DUMPING

Unwanted background from the target region is mainly due to primary particles, with large betatron amplitudes, hitting the target support or the vacuum chamber near to it. Figure 7 illustrates the technique used for

dumping such particles on the vacuum chamber in the area opposite the target position. The necessary closed-orbit deformation is obtained by energizing suitable pairs of CPS kicker magnets⁴.

Using this technique, the ratio of secondary particles, from the target support and vicinity, to the secondaries from the target has been decreased by a factor of 20. Radioautographs for this comparison are shown in Fig. 8. There is also the possibility of using this technique to cut off the tail of fast bursts.

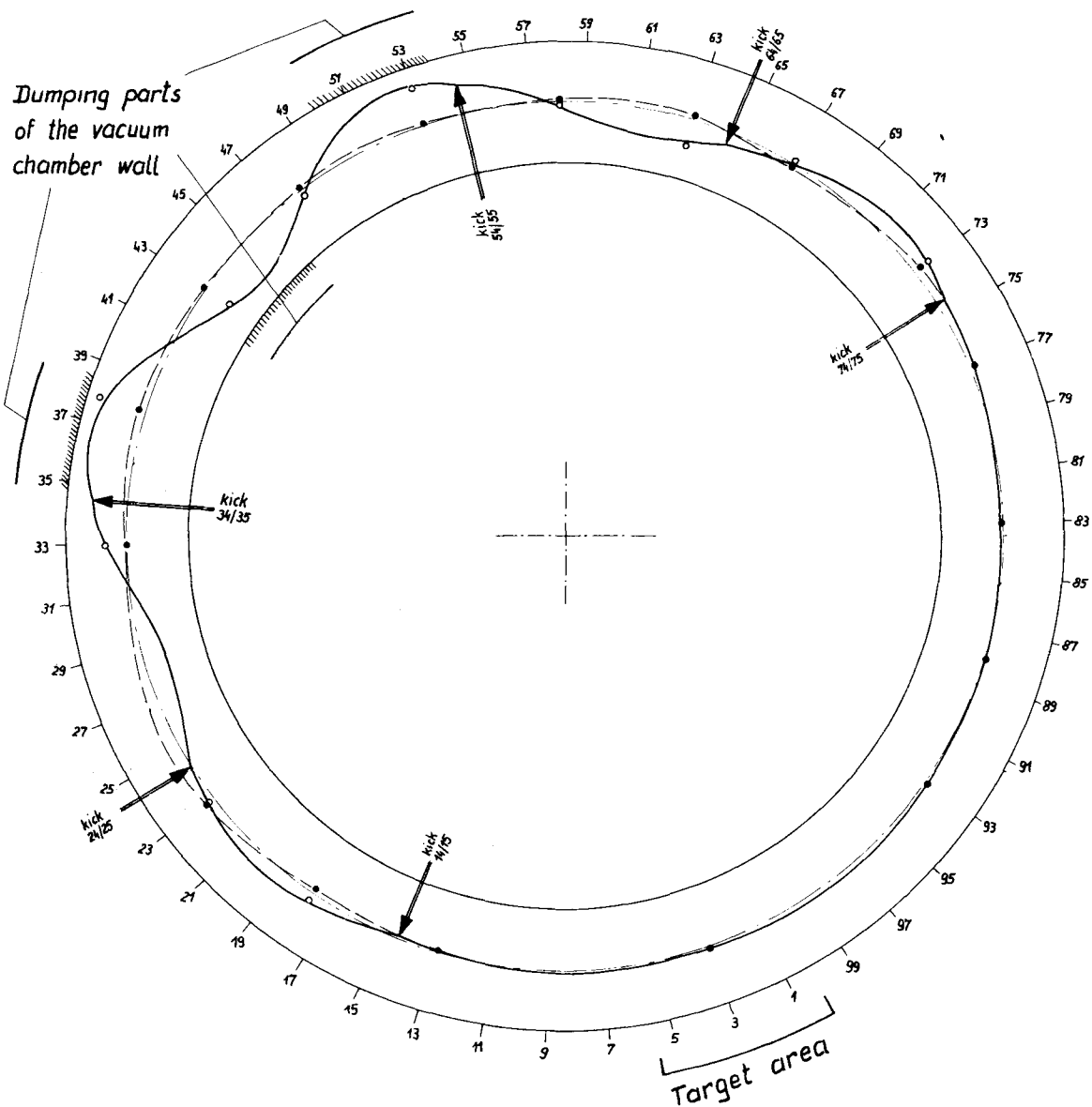


Fig. 7 Closed-orbit deformation to dump scattered protons.

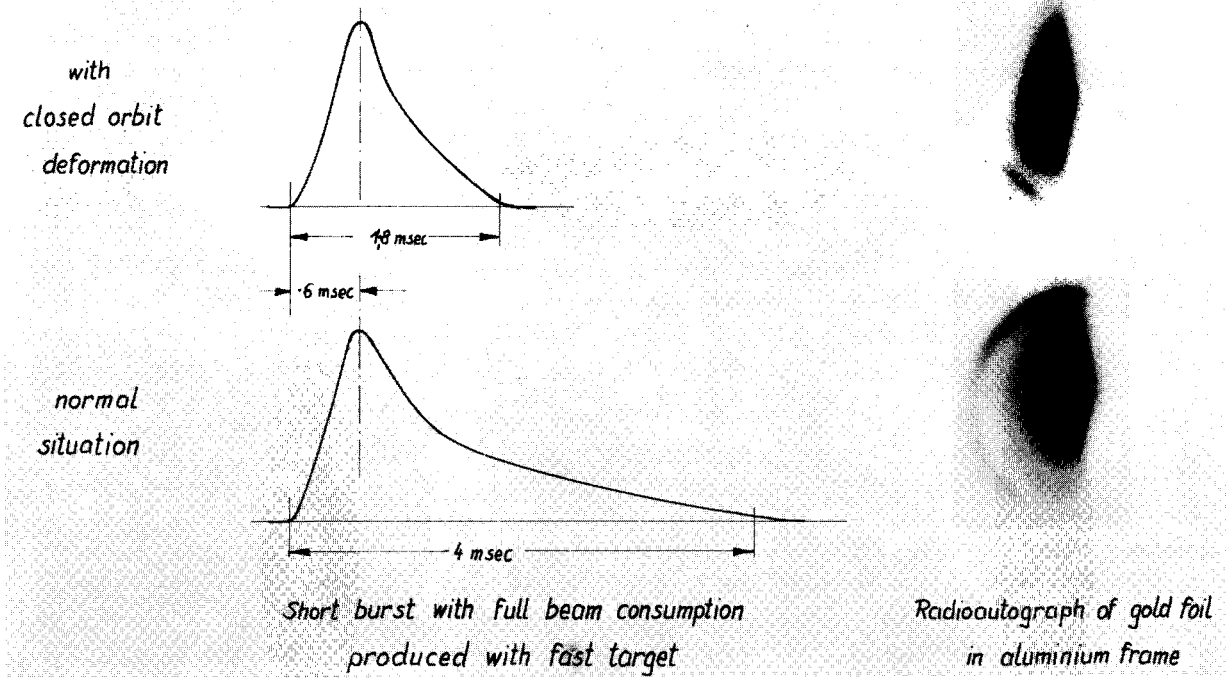


Fig. 8 Effects of dumping. Top: With closed orbit deformation. Bottom: Normal situation.

V. APPENDIX

Symbols

The values in the text are calculated with the the following formulas which are admissible approximations:

$$\Delta\omega/\omega = \Delta E/2E \quad (1)$$

$$E_M = \int_0^{t_c} N_M dt \quad (2)$$

$$i = U_M t/L \quad (3)$$

$$E_r = R \int_0^{t_r} i^2 dt = R(U_M^2/L^2) \int_0^{t_r} t^2 dt = \frac{1}{3} R(U_M^2/L^2) t_r^3 \quad (4)$$

$$\Delta E_r = \Delta E_d = \frac{2}{3} (\Delta U_M/U_M) R (U_M^2/L^2) t_r^3 \leq \pm 1 \times 10^4 \text{ joules} \quad (5)$$

$$\Delta E_f = 2(\Delta U_M/U_M) R (U_M^2/L^2) t_r^2 t_f \leq \pm 1 \times 10^4 \text{ joules (for } t_f = 0.3 \text{ s)} \quad (6)$$

$$\Delta E = \Delta E_M + \Delta E_r + \Delta E_f + \Delta E_d = \pm 4 \times 10^4 \text{ joules} \quad (7)$$

$$\frac{\Delta\omega}{\omega} = \frac{\Delta E}{2E} = \pm 1.3 \times 10^{-4} \quad (8)$$

- ω = mean revolution frequency
- E = 1.5×10^8 joules = energy stored in the flywheel
- ΔE = energy difference in the flywheel between successive machine cycles
- $t_c \leq 5$ s = time of machine cycle
- $t_r \leq 1.2$ s = rise time of magnetic field
- t_f = time of flat top of magnetic field
- $t_d \leq t_r$ = time of decrease of magnetic field
- N_M = driving power of the motor
- E_M = energy gain of the driving motor during one machine cycle
- E_r = energy loss in the magnet coil during t_r
- E_f = energy loss in the magnet coil during t_f
- E_d = energy loss in the magnet coil during t_d
- L = 0.9 h = inductivity of the CPS magnet
- R $\approx 0.3 \Omega$ = resistance of the CPS magnet
- U_M $\approx 5,400$ v = magnet voltage
- i $\leq 6,000$ amp = magnet current

VI. ACKNOWLEDGEMENTS

A major contribution to target development has been made by M.G.N. Hine. In addition, a large part of the CERN-PS Machine Division has joined in the work on target techniques.

K.H. Reich started target development and brought into use the basic target system. Th. Sluyters developed the counter monitors and completed the target system.

The development of the mean-speed regulation, and the measurements, were carried out in collaboration with H. Hödle, Brown Boveri Company, Baden, and M. Georgijevic, CERN-PS Machine Division. Ch. Brooks and P.B. Mulder developed the electronic equipment. Thanks are due to F. Grütter for helpful discussion.

REFERENCES

1. M. GEIGER, *Basic Relations Concerning RF Excitation of Batatron Oscillations in the CPS*, CERN-PS/Internal Report RF 59-2.
2. *Brown Boveri Review*, vol. 46, No. 6 (1959).
3. J. A. GEIBEL, *Results of Measurements with the Fast Large Foil Target*, CERN-PS/Internal Report, AL 61-8.
4. M. G. N. HINE, *Operation of Internal Targets in the CPS for Counter Experiments*, PS/Int. TH 60-1.
5. E. REGENSTREIF, *The CERN Proton Synchrotron* (1st and 3rd part), CERN 59-29, 61-9.
6. M. G. N. HINE, Features of the CERN Proton Synchrotron of Interest to Experimenters, *Proceedings of International Conference on Instrumentation of High-Energy Physics, held at Lawrence Radiation Laboratory, 1960*, Interscience Publishers, New York, 1961.

DISCUSSION

- E. D. COURANT: Could you say a little bit about your measurements of the absolute number of interactions in the target as compared to the number of protons circulating?
- W. Richter: With the large 5-micron aluminum-foil target, which I have shown, we have made a measurement comparing the slope of the burst shape with the theoretical one. From this, Dr. Geibel has calculated that about 60 percent of the circulating protons are effective in making interactions in the target. There is a pertinent internal CERN report, it is CERN P S Internal Report, AL 61-8.
- E. D. COURANT: When you say 60 percent of the protons make interactions, what is your definition of an interaction? The point is, do you include diffraction scattering among interactions in that sense?
- W. RITCHER: No, we don't include diffraction scattering.